Available online at www.sciencedirect.com
ScienceDirect
Journal of Photochemistry and Photobiology A: Chemistry 194 (2008) 318–326
Journal of Photochemistry and Photobiology A:Chemistry
www.elsevier.com/locate/jphotochem

Photoinduced intramolecular charge transfer in methyl ester of *N*,*N*′-Dimethylaminonaphthyl-(acrylic)-acid: Spectroscopic measurement and quantum chemical calculations

Subrata Mahanta, Rupashree Balia Singh, Samiran Kar [1], Nikhil Guchhait *

Department of Chemistry, University of Calcutta, 92 A.P.C. Road, Kolkata 700009, India

Received 28 April 2007; received in revised form 6 August 2007; accepted 28 August 2007
Available online 1 September 2007

Abstract

The excited state intramolecular charge transfer process of a synthesized donor–acceptor naphthalene chromophoric system methyl ester of *N*,*N*′-Dimethylaminonaphthyl-(acrylic)-acid (MDMANA) has been investigated spectroscopically in combination with quantum chemical calculation. Apart from the local emission the molecule shows a solvent polarity dependent low energy emission from the charge transfer excited state. In polar protic solvents ground state hydrogen bonded clusters of MDMANA are formed which also shows low energy emission. Structural calculation and potential energy surfaces along both the donor and acceptor twist coordinates by considering twisted intramolecular charge transfer (TICT) model at density functional theory (DFT) level predict that a stabilized twisting geometry is responsible for charge transfer emission. The solvent polarity effect on the emission spectra has been explored using time-dependent density functional theory-polarizable continum model (TDDFT-PCM) which correlates well with the experimental spectral data.

Keywords: *N*,*N*′-Dimethylaminonaphthyl-(acrylic)-acid methyl ester (MDMANA); Dual fluorescence; Twisted intramolecular charge transfer; Density functional theory

1. Introduction

In the realm of photochemistry, the formation of the charge transfer (CT) state is one of the fundamental processes [1–6]. Research interest was directed towards the CT phenomenon after the first observation of dual fluorescence from 4-(*N*,*N*′-dimethylamino) benzonitrle (DMABN) in polar solvents in 1959 by Lippert et al. [1]. Since then, a variety of systems have been studied to explore the mechanistic insight of dual emission in donor–acceptor CT molecules [1–13]. Apart from the normal fluorescence band (L_b), the origin of the longer wavelength 'anomalous' (L_a) fluorescence band of DMABN was assigned to the formation of the charge transfer state [14]. This process involves relaxation of the solvent dipoles around the fluorophore and the formation of the CT state depends on the dielectric relaxation rate. Grabowski and co-workers proposed twisted intramolecular charge transfer (TICT) model and explain dual emission in a number of systems, e.g. 4-dialkylamino derivates of benzonitrile, benzaldehyde, pyrimidines, pyridine, etc. [15,16]. According to this model, the formation of CT state from the complete decoupling of the donor and acceptor groups is best achieved when the two groups are perpendicular to each other. In this twisted conformation, the dipole moment is greatly enhanced and this leads to greater stability of the CT state with increasing solvent polarity. An alternative planarised intramolecular charge transfer model for the longer wavelength band was put forward by Zachariasse and co-workers in 1993 [17]. According to them, the dual emission of DMABN is originated from the coupling of the NMe_2 group with the quinoid like benzene π system. Apart from the experimental investigation on the charge transfer phenomenon of a number of donor–acceptor systems, theoretical approaches to this problem have also been suggested by many groups [6,18–20]. Ab initio and DFT methods have been applied to explore the potential energy surfaces along the twisting co-ordinates in absence as well as in presence of solvents to throw light on

* Corresponding author.
E-mail address: nguchhait@yahoo.com (N. Guchhait).
[1] Present address: CHEMGEN Pharma International, Dr. Siemens Street, Block GP, Sect. V, Salt Lake City, Kolkata 700091, India.

1010-6030/$ – see front matter © 2007 Elsevier B.V. All rights reserved.
doi:10.1016/j.jphotochem.2007.08.030

the mechanistic path of ICT process [9–12,18–20]. Though different schools put forward different theoretical models, the most accepted one is the TICT model advocated by Grabowski et al. [2,3].

Apart from the basic scientific interest on photoinduced ICT process of donor–acceptor charge transfer systems, the applications of ICT molecules as fluorescence probe are interesting and demanding [21–23]. The sensitivity of the longer wavelength band on local polarity and local viscosity of the surroundings makes the charge transfer chromophore a good fluorescent reporter of the surrounding microenvironment [21–23]. The need and interest for new molecules multiplied due to their vast application in the field of pure and applied sciences such as pH and ion detectors, etc. [24]. The photoinduced ICT process may also play a crucial role in biological light harvesting processes such as photosynthesis [25]. In the present work, we have studied the photophysical properties of the newly designed and synthesized donor–acceptor system methyl ester of *N*,*N*′-Dimethylaminonaphthyl-(acrylic)-acid (MDMANA) containing naphthalene chromophore. The ground and excited state properties of MDMANA have been explored by absorption and emission spectroscopy. Theoretical calculations at DFT level with B3LYP functional and 6-31G basis set were performed to study ground and excited state properties of MDMANA. The potential energy surfaces with respect to twist coordinates for the ground and first two excited singlet states indicates the formation of CT state in the first excited singlet state. The potential energy curves (PEC) with inclusion of solvent effect has been explored in acetonitrile solvent using DFT-PCM and TDDFT-PCM model for the ground and excited states, respectively, to correlate the experimental finding with theoretical results.

2. Materials and methods

2.1. Materials

Methyl ester of *N*,*N*′-Dimethylaminonaphthyl-(acrylic)-acid (Scheme 1) was prepared by stirring a mixture of 4-dimethylaminonaphaldehyde and methyl (triphenylphosphoraxylidene) acetate in dry dichloromethane at room temperature for about 24 h. After the solvent was removed over vacuum, the crude compound was purified on silica gel column chromatography and repeated crystallization in minimum amount of methanol to get pure product of MDMANA, ^{1}H NMR (400 MHz, $CHCl_3$): δ 2.96 (S, 6H, –NMe_2), 3.84 (S, 3H, OMe), 6.46 (d, J = 21 Hz, 1H), 7.07 (d, J = 10.6 Hz, 1H), 7.25–7.58 (m, 2H), 7.72 (d, J = 10.6 Hz, 1H), 8.18–8.21 (m, 1H), 8.26–8.29 (m, 1H), 8.49 (d, J = 21 Hz, 1H).

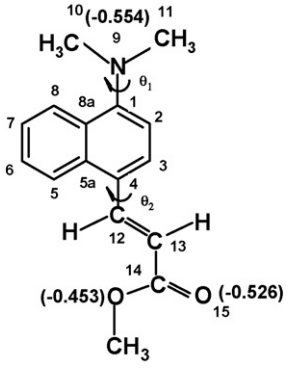

Scheme 1. Structure of MDMANA with atom numbering, θ_1 and θ_2 are donor and acceptor twist angles, respectively. Calculated charge densities are given in parenthesis.

Spectroscopic grade solvents such as hexane (HEX), *n*-heptane (HEP), cylohexane (CYC), methylcyclohexane (MCH), tetrahydrofuran (THF), chloroform ($CHCl_3$), carbon tetrachloride (CCl_4), dioxane (DOX), methanol (MeOH), ethanol (EtOH), *iso*-propanol (*iso*-pr) and acetonitrile (ACN) solvents were purchased from Spectrochem and were used after proper distillation. Sulphuric acid from E-Merck was used after proper vacuum distillation. Triple distilled water was used for the preparation of aqueous solutions.

2.2. Steady state and time-resolved measurements

The absorption and emission spectra were measured by Hitachi UV-VIS U-3501 spectrophotometer and Perkin-Elmer LS-50B spectrophotometer, respectively. In all measurements, the sample concentration was maintained within the range 10^{-4} to 10^{-5} mol/dm^3 in order to avoid aggregation and reabsorption effects.

2.3. Computational procedures

The theoretical global minimum structure of MDMANA and its molecular properties have been calculated using Gaussion 03W software [26]. Structural optimization has been done at DFT level with B3LYP functional and 6-31G basis set. The theoretical potential energy curves (PEC) for the ground and first two excited singlet states have been explored following the twisted intramolecular charge transfer model as proposed by Grabowski et al. [2,3]. So far there are different ways to calculate the ground and excited state surfaces for the donor–acceptor CT systems [27–37]. In our case during the evaluation of the potential energy surface, both in vacuo and in acetonitrile solvent, the structural parameters have been kept frozen to that of optimized geometry of the ground state for all the points and all the states investigated; the only parameter varied is the twisting angle θ_1 for donor group and θ_2 for acceptor group (Scheme 1). The PECs for the first two excited singlet states have been obtained using time-dependent density functional theory (TDDFT). The PECs with inclusion of solvent effect is also constructed using TDDFT-PCM method for the above mentioned basis set. The TDDFT method of calculation using Gaussian 03W does not implement analytical gradients within TDDFT and hence it fails to optimize the geometries for the excited states. Though TDDFT method of calculation fails to optimize the geometries for the excited states, results obtained using this method correlates well with the experimental data [9–12,27–31].

3. Results and discussions

3.1. Absorption spectra

The absorption spectra of MDMANA (Fig. 1a) measured in different solvents show a single broad band at ~358 nm in non-polar solvents which shows slight sensitivity to solvent polarity, shifting to ~363 nm in ACN. This absorption band is nothing but the ππ* transition of naphthalene chromophore. However, this dependence of wavelength maxima on solvent polarity is not linear, since in case of water, the position of absorption maxima is blue-shifted to ~354 nm. Very recently, we have found that the absorption peak is blue shifted in case of some donor–acceptor charge transfer systems in protic solvents [9–12]. The spectral data are presented in Table 1. This exception to the trend observed in case of water may be due to the strong hydrogen bonding capability of water. Structurally the molecule MDMANA has several sites suitable for hydrogen bond formation with protic solvents. Therefore, the absorption band at ~354 nm may arise from the hydrogen bonded solvated complex of MDMANA (Scheme 2). Other polar protic solvents such as ethanol, methanol the absorption band appears at the red side with respect to the absorption band in hexane. This is because the hydrogen bonding strength of ethanol and methanol solvent is comparatively less and hence these solvents do not shift the absorption band position to the blue as is observed in water.

It is found that the donor–acceptor charge transfer systems show characteristics spectral change in presence of acid. As shown in Fig. 1b, addition of dilute H_2SO_4 in MeOH solution results in the generation of a new band at ~313 nm at the expense of ~363 nm band. Although there are several possible protonation sites in the molecule, protonation at the lone pair of nitrogen of tertiary amino group favours over other sites. The calculated negative charge density at the nitrogen atom (−0.554) is higher than that of the oxygen atoms (−0.453 and −0.526) for the global minimum structure (Scheme 1). Hence the protonated species can be formed on addition of acid as per Scheme 3 and the absorption band is blue shifted due to less resonance stabilization of the protonated species than its neutral counter part.

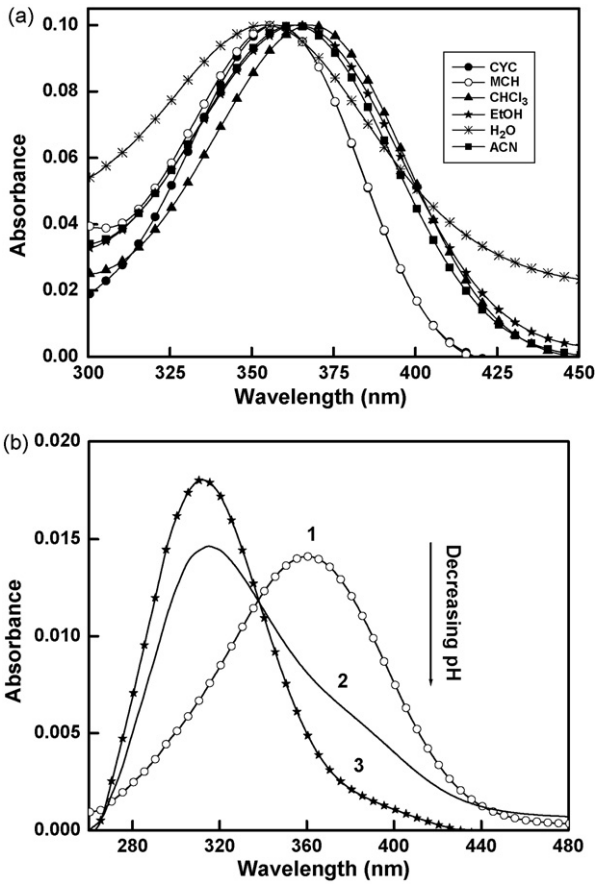

Fig. 1. (a) Absorption spectra of MDMANA in different solvents of varying polarity at room temperature and (b) the absorption spectra of MDMANA with addition of dil. H_2SO_4 in MeOH: (1) without acid and (2–3) with decreasing pH.

Table 1
Absorption and emission maxima (nm) and quantum yields of different bands of methyl ester of *N*, *N*′-dimethylaminonaphthyl-(acrylic)-acid (MDMANA) in different solvents at room temperature

Solvent	Absorption maxima (nm)	Fluorescence band (nm)		φ_{LE}[a]	φ_{CT}[a]	$\bar{\nu}_a$ (cm^{-1})	$\bar{\nu}_f$ (cm^{-1})	($\bar{\nu}_a - \bar{\nu}_f$) ($cm^{-1}$)
		λ_{LE}	λ_{CT}					
HEX	358	–	450	–	0.95	27,933	22,222	5,711
HEP	358	–	450	–	1.19	27,933	22,222	5,711
MCH	358	–	450	–	1.26	27,933	22,222	5,711
CCl_4	362	425	461	0.31	1.47	27,624	21,692	5,932
$CHCl_3$	362	425	466	0.39	2.49	27,624	21,459	6,165
DOX	364	425	472	0.60	2.76	27,473	21,186	6,287
THF	363	425	475	0.49	2.62	27,548	21,053	6,495
Iso-pr	364	423	488	0.28	2.81	27,473	20,492	6,981
EtOH	364	423	498	0.31	2.89	27,473	20,080	7,393
MeOH	363	425	504	0.29	3.05	27,548	19,841	7,707
MeOH + H^+	313	411	504	–	–	31,949	19,841	12,108
ACN	363	428	493	0.36	3.02	27,548	20,284	7,264
Water	354	425	521	0.03	0.14	28,249	19,194	9,055

[a] Quantum yield are of the order of 10^{-3}.

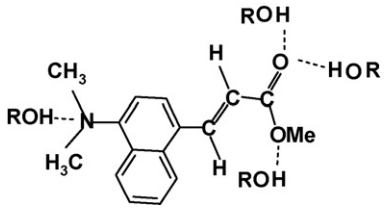

Scheme 2. Possible hydrogen bonded clusters of MDMANA (R = –H, $–CH_3$, $–C_2H_5$, $–C_3H_7$, $–C_4H_9$).

Compared to other reported CT systems the absorbance bands in neutral and acidic medium at ∼363 nm and ∼313 nm, respectively, may be assigned to the neutral and protonated species of MDMANA.

3.2. Emission spectra

The fluorescence emission spectra of MDMANA in different solvents are shown in Fig. 2a and the observed band maxima at room temperature are given in Table 1. In case of non-polar solvents, a single broad emission band at ∼450 nm is observed upon excitation at ∼358 nm absorption band. Whereas in case of polar solvents such as acetonitrile and water dual fluorescence is observed for the same excitation. One higher energy band at ∼425 nm and another solvent polarity dependent lower energy band which ranges between 461 nm in CCl_4 solvent to 521 nm in water. Interestingly, the emission spectra in β-CD shows distinctly two bands—one for the purely LE emission (425 nm) and another for the CT emission (521 nm). This is because β-CD molecule has two type of microenvironment—a non-polar and a hydrophilic part. This observation clearly indicates that in non-polar cyclohexane type of solvent the single broad emission band may compose of LE and CT emission or only the CT emission. Comparing with other similar type of studied systems [9–13,38,39], the higher energy weak band is assigned to the emission from the locally excited (LE) state and the lower energy strong emission band arises from the charge transfer (CT) state. Apparently the red shifting of this anomalous low energy band is found to be dependent on solvent polarity. The absence of mirror symmetry in the absorption and emission spectra in polar solvents predicts that the ground and excited state of the molecule are of different geometries. The excitation spectra (Fig. 2b) of MDMANA for both the emission bands are found to be independent of excitation wavelength and resemble to the absorption spectra. This indicates that both LE and CT bands originate from the same ground state species which absorbs at ∼358 nm.

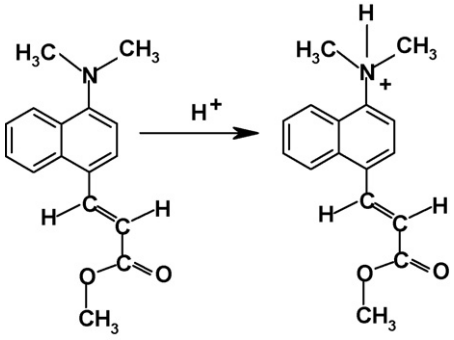

Scheme 3. Protonation at the nitrogen lone pair of MDMANA.

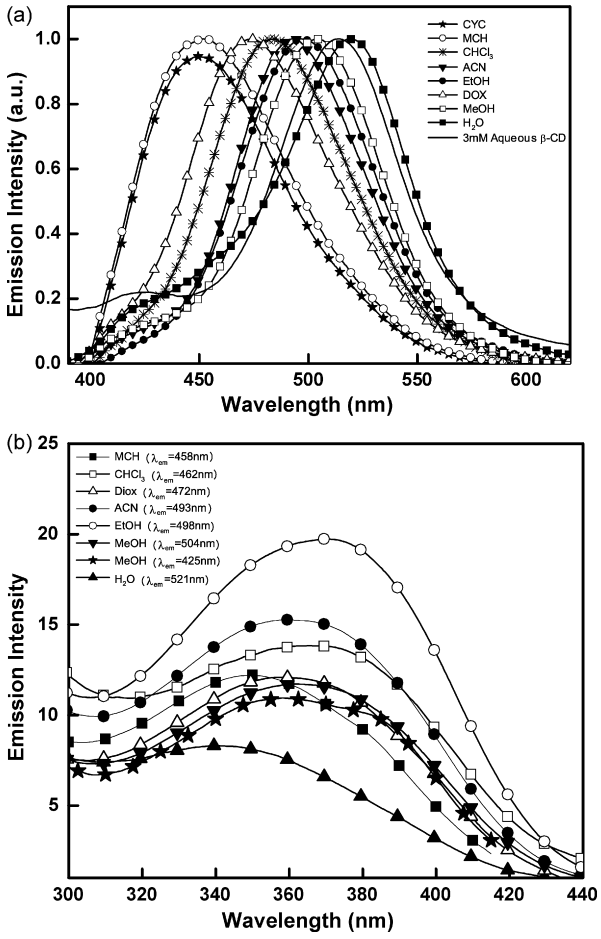

Fig. 2. (a) Fluorescence emission spectra of MDMANA in different solvents at room temperature (λ_{ext} = 358 nm) and (b) excitation spectra of MDMANA in different solvents at room temperature.

Solvatochromic studies of the red-shifted band indicate that the red-shifted emitting species must possess a larger dipole moment compared to the ground state species. This enhancement of the dipole moment in the excited state compared to the ground state is responsible for the stabilization of the CT state with increasing solvent polarity and the solvent dipoles reorient themselves around the fluorophore to attain an energetically favourable arrangement. As usual ways the Lippert–Mataga plot of Stokes shift ($\Delta\nu$) versus solvent parameter $\Delta f(\varepsilon_r, n)$ is shown in Fig. 3a. Following is the Lippert–Mataga relation [40]:

$$\overline{\nu}_a - \overline{\nu}_f = \frac{(\mu^* - \mu)^2}{2\pi\varepsilon_0 hc\rho^3}\Delta f(\varepsilon_r, n)$$

where $\Delta f(\varepsilon_r, n) = [(\varepsilon_r - 1)/(2\varepsilon_r + 1)] - [(n^2 - 1)/(2n^2 + 1)]$.

$\overline{\nu}_a$ and $\overline{\nu}_f$ correspond to the absorption and emission wave number (cm^{-1}), respectively in a solvent with dielectric constant ε_r and n is the refractive index of the medium. The terms h, ε, c and ρ are Planck's constant, permittivity of vacuum, velocity of light and radius of solvent cavity (ρ), respectively. The value of ρ and μ are 4.89 Å and 4.72 D, respectively, for the

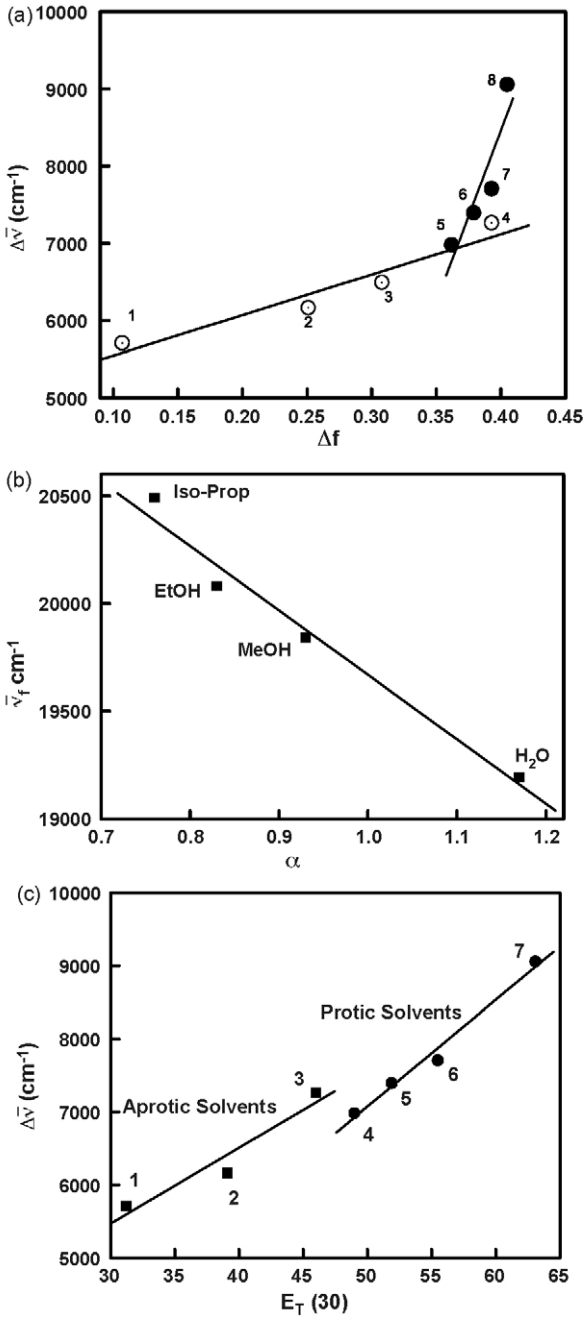

Fig. 3. (a) Plot of Stokes shift ($\Delta\overline{\nu}$) vs. solvent polarity parameter (Δf) (1) hexane, (2) $CHCl_3$, (3) DOX, (4) ACN, (5) *iso*-propanol, (6) EtOH, (7) MeOH and (8) water, (b) plot of emission band maxima of red-shifted band vs. hydrogen bonding parameter, α and (c) plot of stokes shift vs. $E_T(30)$: (1) hexane, (2) $CHCl_3$, (3) ACN, (4) *iso*-propanol, (5) EtOH, (6) MeOH and (7) water.

ground state global minimum structure calculated at DFT level with 6-31G basis set and B3LYP functional. It is found that the plot of Stokes shift ($\Delta\overline{\nu}$) versus Δf shows linearity for non-polar and polar aprotic solvents. From the ratio of the slope and $(\mu^* - \mu)^2/2\pi\varepsilon_0 hc\rho^3$ of the Lippert–Mataga plot, the excited state dipole moment is obtained to be 7.5 D. This large change in dipole moment from the ground to the excited state occurs due to atomic charge redistribution in the excited state and this occurs by charge transfer from the electron rich donor moiety (–NMe_2 group) to the acceptor moiety (ester group). High excited state dipole moment by charge redistribution leads to a solvent polarity dependent red-shifted emission due to different extent of stabilization of the molecule in the excited state.

In case of polar protic solvents with hydrogen bonding capacity a deviation from linearity is observed in the Lippert–Mataga plot indicating that H-bonding has some role for the red-shifted emission band. Cazeau-Dubroca et al. [41] proposed that the tetragonal arrangement of amine side due to formation of H-bond with protic solvents in the ground state favours the ICT process [9–13]. In protic solvents, it is found that the emission band position ($\overline{\nu}_f$) of the red-shifted band varies linearly with the hydrogen bonding parameter α (Fig. 3b) [42]. This indicates that the red-shifted emission band in polar protic solvent arises from the CT emission of the hydrogen bonded clusters of the studied molecule. Overall, the red-shifted emission band shows its dependence on both the polarity and on the hydrogen bonding capability of the solvent. Such type of interactions can be distinctly discriminated when the Stokes shift of the band is mapped against solvent polarity parameters $E_T(30)$. The plot of Stokes shift ($\Delta\overline{\nu}$) versus solvent polarity parameter $E_T(30)$ is shown in Fig. 3c. It can be seen from the figure that there are two types of slope for aprotic and protic solvents. This indicates that in case of protic solvents, the variation of position of emission maxima is mainly influenced by hydrogen bonding capability and in aprotic solvent the CT emission is influenced by dipolar interaction.

Addition of dilute H_2SO_4 to the methanolic solution of MDMANA (Fig. 4) shows an increase in intensity at the position of LE band with decrease in intensity of the CT band. As per the calculated negative charge density, the preferred protonation site at the lone pair of the dimethylamino group (–NMe_2) hinders the formation of the CT state and H-bonded clusters, thereby decreasing intensity of red sided CT emission. The high energy emission band at 411 nm is therefore assigned to emission from the locally excited state of the protonated species. However, at high acid concentration, the presence of red-shifted emission band along with the LE emission of the

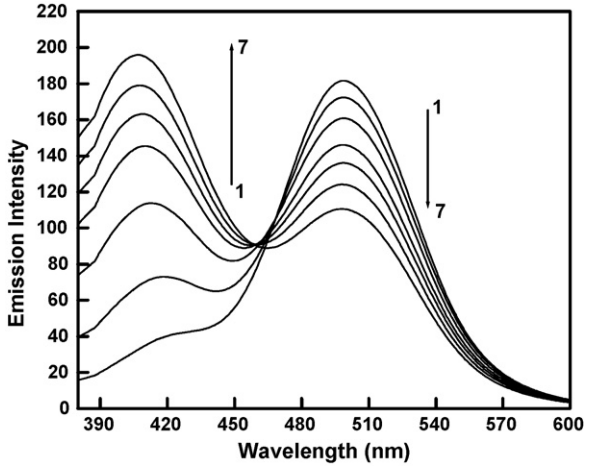

Fig. 4. Effect of dil. H_2SO_4 on the emission spectra of MDMANA in MeOH ($\lambda_{ext.}$ = 313 nm). Arrow indicates decrease of pH.

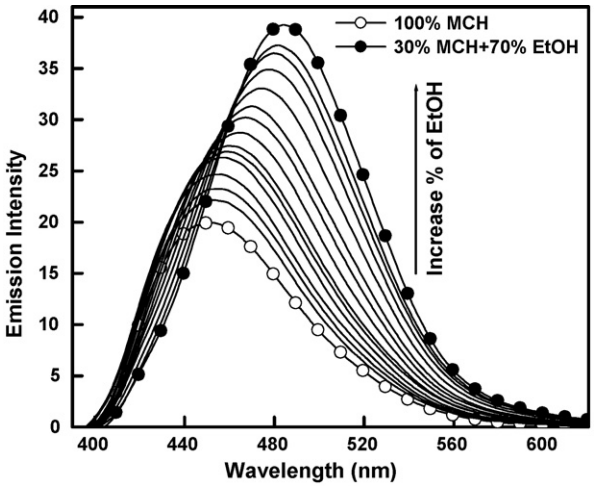

Fig. 5. Effect of addition of EtOH on the emission spectra of MDMANA in MCH at room temperature (λ_{ext} = 358 nm).

protonated species indicates that deprotonation may occur in the excited state potential energy surface resulting in some CT emission.

The emission spectra of MDMANA in binary solvent mixture of methylcyclohexane and ethanol are presented in Fig. 5. Addition of EtOH in MCH solution of MDMANA shows a red shift of the emission band from ~440 nm to ~480 nm with increasing intensity. This observation also indicates that the CT state originates from the LE state on addition of EtOH to MCH solution. The solvent reorientation leads to this characteristic solvatochromic red shift. The fluorescence intensity of the CT band in MeOH increases due to higher fluorescence quantum yield of the CT band in methanol solvent than in hexane solvent (Table 1).

3.3. Computational details

The first insight into the electronic reorganization during the process of charge transfer can be achieved by the determination of the ground state global minimum structure of MDMANA. The trans form with respect to C_{12}–C_{13} double bond (Scheme 1) was found to be the most stable or the lowest energy structure due to absence of steric hindrance as compared to the cis form. In the calculated structure of MDMANA, the –NMe_2 group is found to be out of plane ($\angle C_{11}$–N_9–C_1–C_2, $\theta_1 = 24.39^\circ$) of the aromatic ring and the N-atom of the NMe_2 group is pyramidal in its global minimum state in vacuo. Very similarly the acceptor group is also titled ($\theta_2 = 22.09^\circ$) with respect to the aromatic ring and hence the π-orbitals of acceptor is not in parallel to the aromatic π-orbitals. Optimized parameters are given in Table 2. Such twisted geometry at the donor and acceptor groups arises due to steric hindrance caused by 'Peri' hydrogen of naphthalene ring. As per TICT model it is expected that such pre-twisted geometry favours excited state ICT reaction for donor–acceptor system. The PESs along the donor and acceptor twist coordinates have been evaluated at DFT level for the ground and first two excited states. As shown in Fig. 6, twisting of the donor group leads to increase in energy, with a maximum

Table 2
Ground state optimized geometrical parameters of MDMANA at DFT level with B3LYP functional and 6-31G basis set

Bond lengths	Value (Å)	Angles	Value (°)
C_{10}–N_9	1.475	$\angle C_{10}$–N_9–C_{11}	112.85
C_{11}–N_9	1.464	$\angle C_{10}$–N_9–C_1	118.93
N_9–C_1	1.414	$\angle C_{11}$–N_9–C_1	118.43
C_1–C_2	1.393	$\angle C_4$–C_{12}–C_{13}	126.16
C_2–C_3	1.404	$\angle C_{13}$–C_{14}–N_{15}	124.03
C_3–C_4	1.393	$\angle C_{11}$–N_9–C_1–C_2	24.39 (θ_1)
C_4–C_{12}	1.461	$\angle C_3$–C_4–C_{12}–C_{13}	−22.09 (θ_2)
C_{12}–C_{13}	1.354		
C_{13}–C_{14}	1.461		
C_{14}–O_{15}	1.243		

Numbering of atoms as per Scheme 1.

at $\theta_1 = 74^\circ$ for the S_0 state in vacuo. Then a slight decrease in energy is observed up to $\theta_1 = 94^\circ$ followed by an abrupt increase in energy. This peculiar observation can be well accounted for, if the 'Peri Effect' between the donor group and H-atom at the

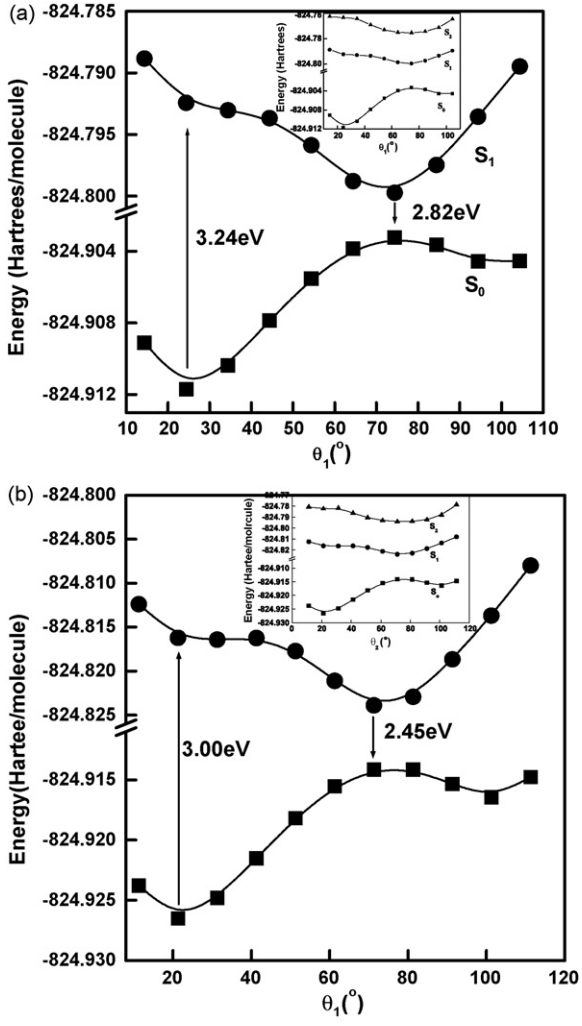

Fig. 6. Potential energy curves for ground and first excited singlet state of MDMANA with varying of donor twist angle (θ_1) in (a) vacuo and (b) in ACN solvent. Insets show the combined view of the ground and first two singlet excited states in vacuo and in ACN.

C_8 position of the naphthalene ring is taken into consideration (Scheme 1). During the course of twisting, the donor group feels some steric interaction with this Peri H-atom and the conformer becomes unstable. This also accounts for the initial twist of the $-NMe_2$ group out of plane in the global minimum state. Such type of interaction is absent in benzene type of systems and hence the donor group is nearly planar in its global minimum state [9–12]. For the evaluation of the first two excited single state PECs, TDDFT method with B3LYP functional and 6-31G basis set is used. As can be seen in Fig. 6a, the energy of the first excited state (S_1) decreases and attains a minimum at $\theta_1 = 74^\circ$. The second excited state (S_2) also shows a similar minimum at $\theta_1 = 74^\circ$ but excitation to the second excited state requires far more energy than that for the first excited state, therefore, the phenomenon of TICT occurs in the S_1 state. Over all PESs for the ground and excited state are of asymmetric double well type. However, in the S_1 surface, the fully twisted geometry is the minimum energy structure and is responsible for red-shifted emission. The inclusion of solvent effect using DFT/PCM model shows that the $-NMe_2$ group is 21° out of plane of the aromatic ring in the ground state global minimum. The evaluation of PECs in acetonitrile solvent using PCM model (Fig. 6b) shows a similar variation of energy along the twist co-ordinate with a maximum at $\theta_1 = 71^\circ$. The nature of the PECs for both the ground and the excited states are basically the same as obtained in vacuo. The twisted conformer in the S_1 state however becomes more stable in presence of solvent by ~15.17 kcal/mol. Twisting of the acceptor group (θ_2) in vacuo as well as in ACN solvent (Fig. 7a and b) also shows slight different potential energy variation and the energy maxima are found at acceptor twist angle of 87° and 93° in vacuo and in ACN solvent, respectively. Although acceptor rotation can provide red-shifted emission, but the transformation from LE to CT state passes through an energy barrier (barrier energy 2.25 kcal/mol in vacuo and 1.66 kcal/mol in ACN) in the S_1 surface. In addition, the CT state in the S_1 surface is higher in energy than the LE state. Therefore, donor twisting favours over acceptor twisting path for the charge transfer process in the excited state. The variation of oscillator strength and vertical excitation energy for the S_1 state in vacuo and ACN solvent is shown in Fig. 8a and b, respectively. As shown in Table 3 and Fig. 8, the experimental absorption and emission energies in vacuo and ACN solvent matches reasonably well with theoretical values obtained from donor twisting instead of acceptor twisting. The experimentally observed emission energy in ACN solvent (2.52 eV, 493 nm) matches well with that obtained theoretically in ACN solvent for donor group rotation (2.45 eV,

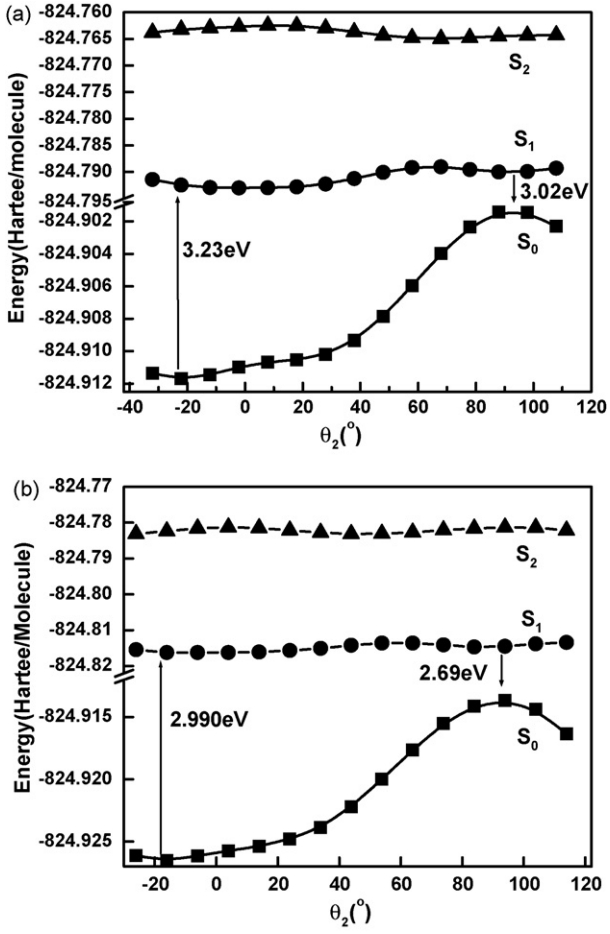

Fig. 7. Potential energy curves for ground and first two excited singlet states of MDMANA with varying of twist angle, θ_2 for acceptor group rotation (a) in vacuo and (b) ACN solvent.

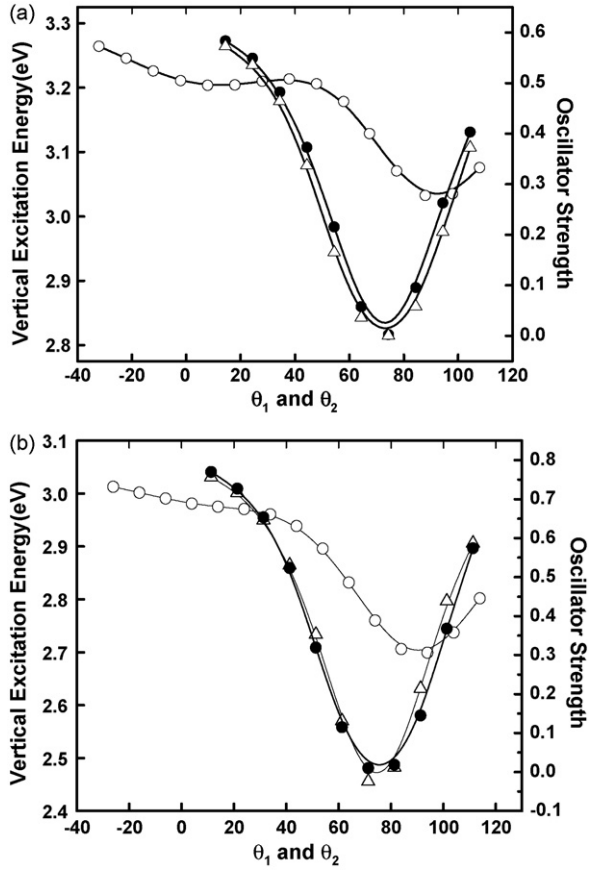

Fig. 8. The variation of oscillator strength (●) and vertical excitation energies (△) with varying donor twist angle (θ_1) and vertical excitation energies (◯) with variation of acceptor twist angle (θ_2) of MDMANA in (a) vacuo and (b) in ACN solvent.

Table 3
Comparison of experimental spectral data with theoretical values of vertical transition energies (eV) of MDMANA in vacuo and ACN solvent computed at DFT level (ways of calculation are given in the experimental section)

Medium	States	Absorption (eV)		Emission (eV)		
		$E_{exp.}$	$E_{theo.}$	$E_{theo.}$[a]	$E_{theo.}$[b]	E_{exp}
Vacuo	S_1	3.46	3.24 (0.5356)[c]	2.82 (0.0006)	3.03 (0.0015)	2.76[d]
	S_2	–	4.04 (0.0178)	3.48 (0.3895)	3.73 (0.1786)	–
ACN	S_1	3.42	3.00 (0.7275)	2.45 (0.0099)	2.69 (0.0064)	2.52
	S_2	–	3.92 (0.0205)	3.27 (0.4832)	3.60 (0.2267)	–

[a] Donor group twisting.
[b] Acceptor group twisting.
[c] Oscillator strength given in parenthesis.
[d] In *n*-hexane.

507 nm). The theoretical value for emission energy in vacuo (2.82 eV, 441 nm) is very well in agreement to that obtained experimentally in *n*-hexane solvent (2.76 eV, 450 nm). Thus, the stabilized CT state in polar solvent predicts a red-shifted emission which is observed experimentally too. Thus, the theoretical calculations correlate the experimental findings to a large extent.

The HOMO–LUMO molecular orbital picture shows that for the global minimum state (Fig. 9a), the π cloud density is more or less uniformly distributed over the entire π system of the

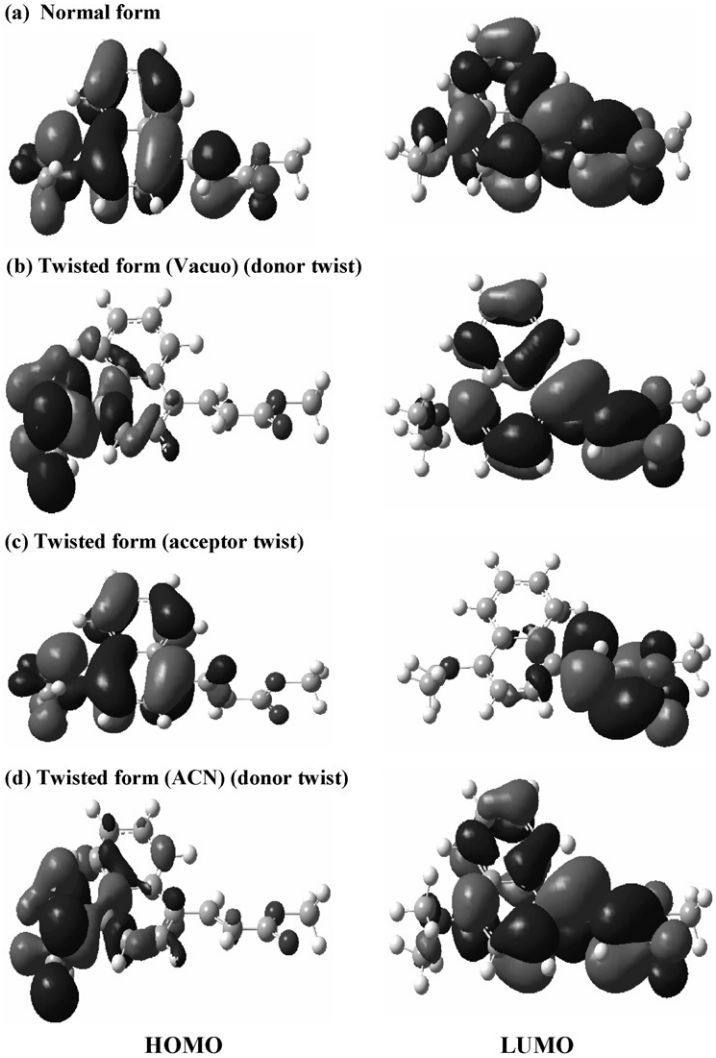

Fig. 9. Molecular orbital pictures (HOMO and LUMO) of MDMANA for the (a) normal, (b) donor twisted, (c) acceptor twisted geometry in vacuo and (d) donor twisted geometry in ACN solvent.

naphthalene ring for both in HOMO (π) as well as in LUMO (π^*). Hence the transition is of π–π^* type which is allowed. Whereas in the twisted state (Fig. 9b and d), the electron density is over N-atom for the HOMO (*n*) and the electron density over the donor N-atom in the LUMO (π^*) becomes practically nil and the acceptor group has reasonable cloud density over it. Thus the transition is the forbidden n–π^* type. This is also revealed from the oscillator strength values which decrease from 0.7347 in the global minimum state to 0.0103 (Fig. 8b) in the twisted state in ACN, i.e. moving from allowed to forbidden transition. Though n–π^* transition is symmetry forbidden, it is considered that the excited state vibronic coupling is responsible for the gaining of emission intensity of the CT emission [3]. On the other hand, the HOMO for the acceptor twisting path show delocalized electron density and the orbital pictures are similar to that of the global minimum structure. This type of delocalized orbital pictures does not support CT process for acceptor twisting path. Therefore, a localized lone pair at the nitrogen centre for donor twisting path is responsible for the phenomenon of TICT in the S_1 state of MDMANA.

4. Conclusion

The molecule MDMANA has been synthesized and its photophysical behaviors have been studied spectroscopically in solvents of varying polarity. The spectral characteristics of MDMANA with variation of the nature of solvents and pH of the medium helps to establish the existence of three types of species in the excited state—a normal excited state species whose emission is insensitive to solvent polarity, a twisted conformer which gives rise to solvent polarity dependent large Stokes shifted emission and a hydrogen bonded solvated complex whose red-shifted emission correlates well with solvent hydrogen bonding parameter. Calculation shows that both the donor and acceptor groups are pre-twisted in the global minimum structure. Theoretical calculations at DFT level using twisted intramolecular charge transfer (TICT) model predict that the LE state relaxes to the CT state along the donor twisted coordinate in the first excited state potential energy surface which leads a red-shifted emission. Exploration of the PECs using time-dependent density functional theory-polarizable continum model (TDDFT-PCM) correlates well the solvent polarity dependent red-shifted CT emission band.

Acknowledgements

NG gratefully acknowledges the financial support received from Department of Science and Technology, India (Project No. SP/S1/PC-1/2003). SM and RBS thank CSIR, New Delhi for senior research fellowship.

References

[1] E. Lippert, W. Luder, H. Boss, in: A. Mangini (Ed.), Advances in Molecular Spectroscopy, Pergamon Press, Oxford, 1962, p. 443.
[2] A. Siemiarczuk, Z.R. Grabowski, A. Krowczynski, M. Asher, M. Ottolenghi, Chem. Phys. Lett. 51 (1977) 315.
[3] Z. Grabowski, K. Rotkiewicz, W. Rettig, Chem. Rev. 103 (2003) 3899.
[4] W. Rettig, Angew. Chem. Int. Ed. Engl. 25 (1986) 971.
[5] J. Herbich, J. Waluk, Chem. Phys. 188 (1994) 247.
[6] A.L. Sobolewski, W. Domcke, Chem. Phys. Lett. 250 (1996) 428.
[7] P. Hazra, D. Chakrabarthy, N. Sarkar, Langmuir 18 (2002) 7872.
[8] J.-S. Yang, K.-L. Liau, C.-M. Wang, C.-Y. Hwang, J. Am. Chem. Soc. 126 (2004) 12325.
[9] A. Chakraborty, S. Kar, N. Guchhait, J. Photochem. Photobiol. A: Chem. 181 (2006) 246.
[10] A. Chakraborty, S. Kar, N. Guchhait, Chem. Phys. 324 (2006) 733.
[11] A. Chakraborty, S. Kar, D.N. Nath, N. Guchhait, J. Chem. Sci. 119 (2007) 195.
[12] A. Chakraborty, S. Kar, N. Guchhait, J. Phys. Chem. A 110 (2006) 12089.
[13] P.R. Bangal, S. Panja, S. Chakravorti, J. Photochem. Photobiol. A: Chem. 139 (2001) 5.
[14] J.R. Platt, J. Chem. Phys. 17 (1949) 484.
[15] Z.R. Grabowski, J. Dobowski, Pure Appl. Chem. 55 (1983) 245.
[16] C. Rulliere, Z.R. Grabowski, J. Dobowski, Chem. Phys. Lett. 137 (1987) 408.
[17] K.A. Zachariasse, M. Grobys, T. von der Haar, A. Hebecker, Y.V. Iiichev, Y.B. Jiang, O. Morawski, W. Kuhnle, J. Photochem. Photobiol. A 102 (1996) 59.
[18] A. Kohn, C. Hattig, J. Am. Chem. Soc. 126 (2004) 7399.
[19] D. Rappoport, F. Furche, J. Am. Chem. Soc. 126 (2004) 1277.
[20] C.J. Jodicke, H.P. Luthi, J. Chem. Phys. 117 (2002) 4157.
[21] F.-Y. Wu, Z.-J. Ji, Y.-M. Wu, X.-F. Wan, Chem. Phys. Lett. 424 (2006) 387.
[22] A. Mallick, B. Haldar, N. Chattopadhyay, J. Phys. Chem. B 109 (2005) 14683–14690.
[23] S. Panja, P. Chowdhury, S. Chakravorti, Chem. Phys. Lett. 393 (2004) 409.
[24] A. Bajorek, J. Paczkowski, Macromolecules 31 (1998) 86.
[25] J.A. Bautista, R.E. Connors, B.B. Raju, R.G. Hiller, F.P. Sharples, D. Goszlota, M.R. Wasielewski, H.A. Frank, J. Phys. Chem. B 103 (1999) 8751.
[26] M.J. Frisch, et al., Gaussian 03, Revision B.03, Gaussian, Inc., Pittsburgh, PA, 2003.
[27] O. Kajimoto, M. Futakami, T. Kobayashi, K. Yamasaki, J. Phys. Chem. 92 (1988) 1347.
[28] W. Rettig, B. Zietz, Chem. Phys. Lett. 317 (2000) 187.
[29] E. Casida, K.C. Casida, D.R. Salahub, J. Quantum Chem. 70 (2002) 933.
[30] Z.I. Cai, J.R. Reimers, J. Chem. Phys. 112 (2000) 527.
[31] O.V. Gritsenko, S.J.A. van Guibergen, A. Gorling, E.J. Baerends, J. Chem. Phys. 113 (2000) 8478.
[32] J. Neugebauer, O. Gritsebko, E. Jan Baerends, J. Chem. Phys. 124 (2006) 214102.
[33] C.J. Jodicke, H.-P. Luthi, J. Chem. Phys. 117 (2002) 4146.
[34] C.J. Jodicke, H.-P. Luthi, J. Am. Chem. Soc. 125 (2003) 252.
[35] R. Cammi, B. Mennucci, J. Tomasi, J. Phys. Chem. A 104 (2000) 5631.
[36] B. Mannucci, R. Cammi, J. Tomasi, J. Chem. Phys. 109 (1998) 2798.
[37] L. Shen, H.-F. Ji, H.-Y. Zhang, Chem. Phys. Lett. 409 (2005) 300.
[38] T. Stalin, N. Rajendiran, Chem. Phys. 322 (2006) 311.
[39] T. Stalin, N. Rajendiran, Chem. Phys. 182 (2006) 137.
[40] E. Lippert, Z. Elecktrochem. Ber. Bunsen-Ges. Phys. Chem. 61 (1957) 962.
[41] C. Cazeau-Dubroca, S. Ait Lyazidi, P. Cambou, A. Peirigua, P. Cazeau, M. Pesquer, J. Phys. Chem. 93 (1989) 2347.
[42] R.W. Taft, M.J. Kamlet, J. Am. Chem. Soc. 98 (1976) 2886.